Investigation of mode structure from BES signals in MAST Upgrade

P. Balazs[1,2], D. Dunai[1], S. Thomas[3], M. Brix[4], S. Hegedus[1], K. Imada[4], J. Galdón-Quiroga[6], C. Michael[5], J. F. Rivero Rodríguez[7], G.I. Pokol[1,2], MAST-U Team[5,*], WPTE Team[8]

[1] *HUN-REN Centre for Energy Research, Budapest, Hungary*

[2] *Institute of Nuclear Techniques, Faculty of Natural Sciences, Budapest University of Technology and Economics, Budapest, Hungary*

[3] *MIT Plasma Science and Fusion Center, Cambridge, MA 02139, USA*

[4] *York Plasma Institute, School of Physics, Engineering and Technology, University of York, Heslington, York YO10 5DD, United Kingdom of Great Britain and Northern Ireland*

[5] *UKAEA (United Kingdom Atomic Energy Authority), Culham Campus, Abingdon, Oxfordshire, OX14 3DB, United Kingdom*

[6] *Departamento de Física Atómica, Molecular y Nuclear, Universidad de Sevilla, Sevilla, Spain*

[7] *Departamento de Ingeniería Mecánica y Fabricación, Universidad de Sevilla, Sevilla, Spain*

[8] *E. Joffrin et al 2024 Nucl. Fusion 64 112019*

**See author list of J. R. Harrison et al., Nucl. Fusion 64, 112017 (2024)*

The Mega Ampere Spherical Tokamak Upgrade (MAST-U) is well-known for hosting a wide variety of MHD phenomena, making it a prime candidate for studying the effects of these phenomena. These efforts are helped by yet another wide range of plasma diagnostics, including beam emission spectroscopy, or BES [1]. On MAST-U, the BES system observes one of the machine's heating beams from a toroidally tangential view with a two-dimensional avalanche photodiode pixel array, making the observation both radially and poloidally resolved on a few-centimeter scale. The goal of the diagnostics is to measure fluctuations in beam emission caused by plasma density fluctuations, which is made possible by the 4 MHz sampling rate of the system.

This work presents the analysis of BES signals in the time–frequency domain, based on the NTI Wavelet Tools [2]. The capabilities are demonstrated through a short study of two common phenomena at MAST-U. The first, fishbones, are fast-particle-driven rapid bursts of MHD activity that can occur when neutral beam heating is used. The second, ELM precursors, are radially localized, coherent MHD oscillations that appear at the plasma edge just before an ELM burst. The selected discharge for the analysis (#50936) featured both effects. It was part of the MU04-EST-04 experiment, performing elongation, triangularity and squareness scans to investigate the impact of high shaping on H-mode and pedestal. The double null plasma was heated by both beams with a total of 3.5 MW power, and the maximum plasma current was 750 kA with a density around $3 \cdot 10^{20}$ m^{-3}, and ion and electron temperatures approximately 1.8 keV and 1 keV, respectively.

The approximate view of the BES system relative to the magnetic surfaces is shown in Figure 1. However, this image does not take into account that the magnetic structure, and therefore any plasma structures elongated along field lines, twist according to the local safety factor. This causes a shift in the effective pixel positions and also smears the emission across

the pixels along field lines. As the finite volume of the beam is illuminated by plasma structures that are elongated along field lines, a pixel collects information from a larger poloidal area when the line of sight and field lines are not quite aligned [3]. Both of these effects are illustrated in Figure 2. The pixels are projected from the image plane along field lines into a poloidal plane. The magnetic smearing is calculated for their center point and plotted with colored curves, where yellow indicates emissions from regions of higher beam current, and therefore higher signal amplitude. These visualizations will help us better understand the results during the analysis.

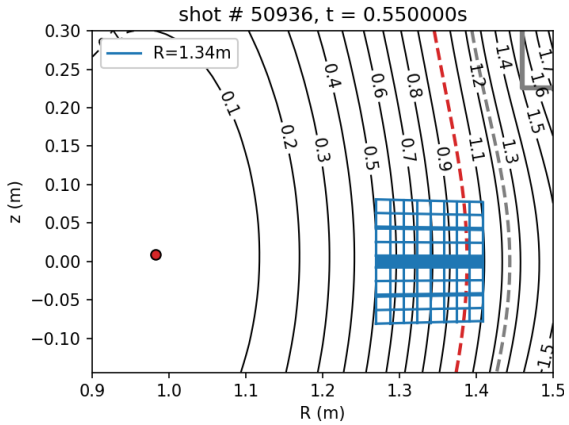

Figure 1. Approximate view of the BES during the flat-top phase of discharge #50936.

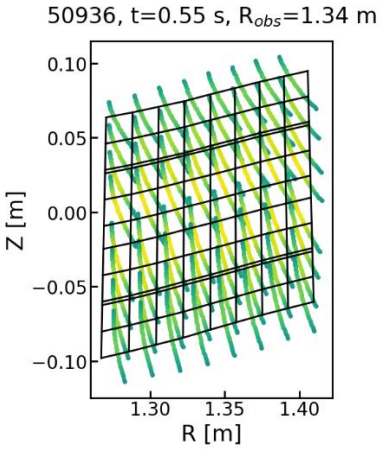

Figure 2. Poloidal localization of pixels and estimations for the magnetic smearing effect.

As the first step of the analysis, Short Time Fourier Transformation (STFT) is calculated using a Gaussian window for one of the BES signals. Figure 3 shows the resulting spectrogram, where both an ELM and a region populated with fishbones are identifiable. Figure 4 shows the fishbones in more detail, with the particular event selected for the study highlighted. For the study of the ELM and its precursor, a handful of raw signals are presented in Figure 5, where the channel in row 4 and column 5 of the array shows particularly strong precursor oscillations. To check this in time-frequency space, an STFT of the same signal in the appropriate area is shown in Figure 6.

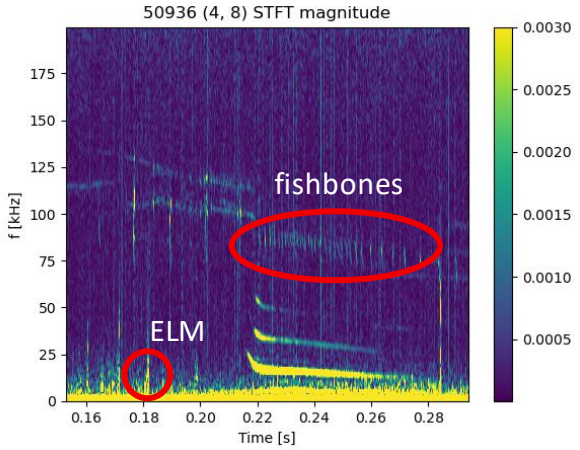

Figure 3 STFT of BES channel (4,8), with both an ELM and fishbones visible in the spectrum.

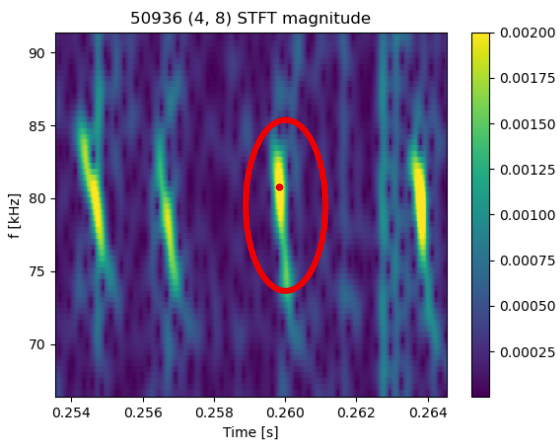

Figure 4 Zoomed-in STFT on the particular fishbone analyzed in the study.

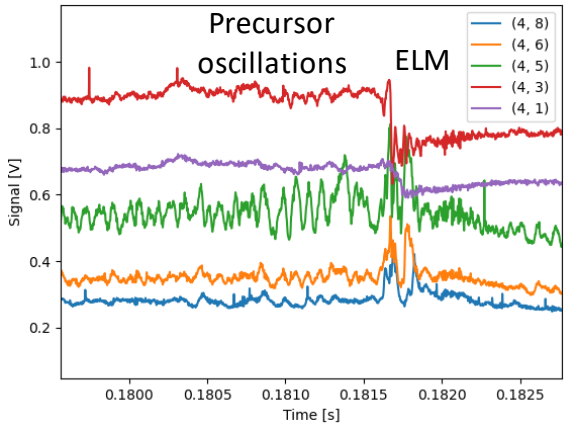

Figure 5. Raw signals of multiple BES channels at the time of the studied ELM. Channel (4,5) shows a strong precursor oscillation.

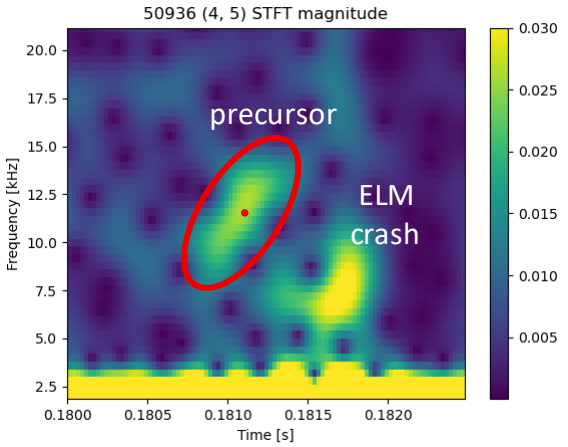

Figure 6. STFT for channel (4,5), showing the ELM crash just after 0.1815 seconds, and the precursor before the crash.

To better localize these events using only BES measurements, the time-frequency points indicated by red dots in Figures 4 and 6 were selected, and their magnitude is plotted for all channels in Figure 7. These show that the signal component due to the fishbone is present in a wide radial range, with larger amplitudes towards the edge. On the other hand, the ELM precursor is well-localized radially. As the next step, the entirety of row 4 and column 5 was selected to study phase relations between channels, with channel (4,5) serving as reference.

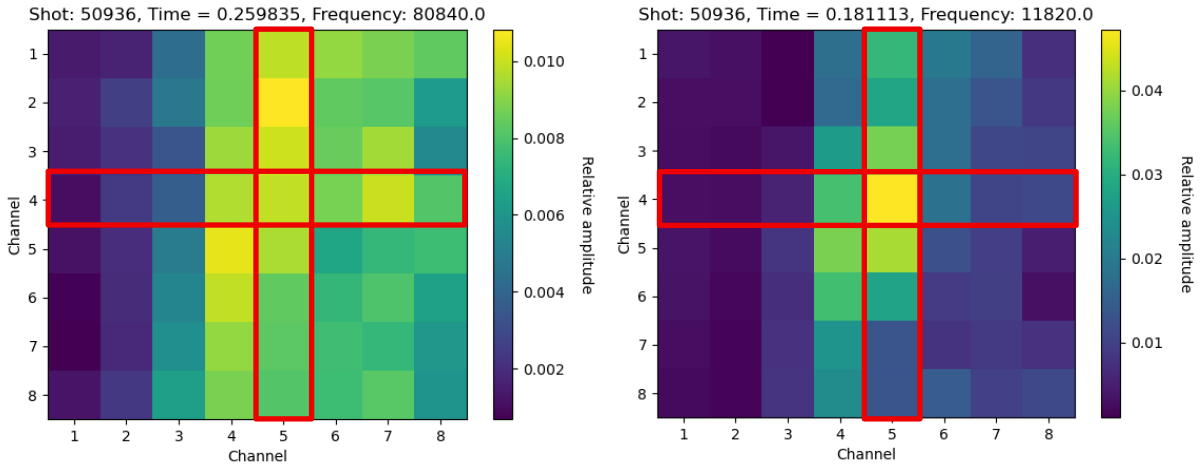

Figure 7. Amplitude of the STFT point taken from the fishbone and ELM precursor. The precursor shows a tighter radial localization.

Figure 8 shows the phases relative to this channel for multiple time-frequency points in close proximity. Relative phases across the row give information about radial phase relations, while the relative phases across the column give information about the poloidal phase relations. In the case of the fishbone, only small phase differences are present. The monotonic trend of the radial phase may be explained by Figure 2, which shows that even the channels of the same detector row have some poloidal distance between them as well.

This work has been carried out within the framework of the EUROfusion Consortium, funded by the European Union via the Euratom Research and Training Programme (Grant Agreement No 101052200 — EUROfusion). Views and opinions expressed are however those of the author(s) only and do not necessarily reflect those of the European Union or the European Commission. Neither the European Union nor the European Commission can be held responsible for them.

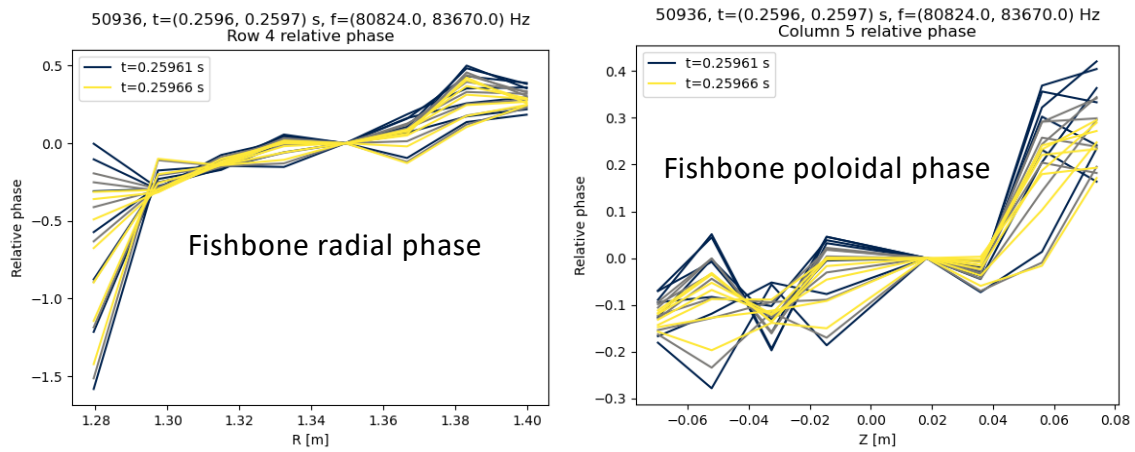

Figure 8. Radial and poloidal phase relations during the fishbone relative to channel (4,5) across row 4 and column 5. The individual curves correspond to a single STFT point from an area around the points selected in Figure 4.

The phase relations, calculated in the same manner for the ELM precursor, are presented in Figure 9. The radial phase in this case shows stronger coherence for the inner channels, while the large and consistent differences in the poloidal phase suggest a well-defined poloidal wavenumber describing the structure. A linear fit reveals this value to be 30.77±0.16 m^{-1}, which corresponds to a wavelength of 0.204±0.001 m.

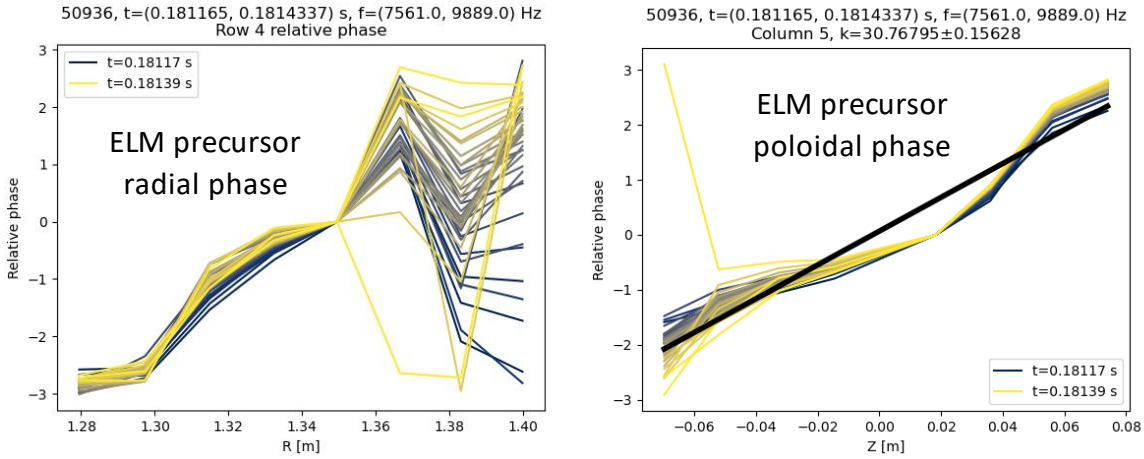

Figure 9. Radial and poloidal phase relations during the fishbone relative to channel (4,5) across row 4 and column 5.

In summary, time–frequency analysis of the MAST-U BES diagnostic system was presented. Two common MHD features were studied as a demonstration: a fishbone-related fluctuation and an ELM precursor. The comparison of the two phenomena first showed that the studied ELM precursor was better localized radially than the fishbone. This is consistent with the relative phases of the mode across row 4 and column 5 of the detector grid not showing major phase differences. During the ELM precursor, however, inner channels radially, including the precursor's radius, are more coherent, and there is a major, consistent phase difference between channels in the poloidal direction. This is indicative of a well-defined vertical wavenumber for the precursor, approximately 30 m^{-1} in this case.

References

[1] Kiss, István Gábor, et al. Fusion engineering and design 86.6-8 (2011): 1315-1318.
[2] https://github.com/fusion-flap/nti-wavelet-tools.git
[3] Balazs, P., et al, Fusion Engineering and Design 216 (2025): 115075.